Model dependence of the ^{2}H electric dipole moment

I. R. Afnan*
School of Chemical and Physical Sciences Flinders University, GPO Box 2100, Adelaide 5001, Australia

B. F. Gibson†
Theoretical Division, Los Alamos National Laboratory, Los Alamos, New Mexico 87545, USA
(Received 12 October 2010; published 16 December 2010)

Background: Direct measurement of the electric dipole moment (EDM) of the neutron is in the future; measurement of a nuclear EDM may well come first. The deuteron is one nucleus for which exact model calculations are feasible. **Purpose**: We explore the model dependence of deuteron EDM calculations. **Methods**: Using a separable potential formulation of the Hamiltonian, we examine the sensitivity of the deuteron EDM to variation in the nucleon-nucleon interaction. We write the EDM as the sum of two terms, the first depending on the target wave function with plane-wave intermediate states, and the second depending on intermediate multiple scattering in the $^3P_1$ channel, the latter being sensitive to the off-shell behavior of the $^3P_1$ amplitude. **Results**: We compare the full calculation with the plane-wave approximation result, examine the tensor force contribution to the model results, and explore the effect of short-range repulsion found in realistic, contemporary potential models of the deuteron. **Conclusions**: Because one-pion exchange dominates the EDM calculation, separable potential model calculations will provide an adequate description of the ^{2}H EDM until such time as a measurement better than 10% is obtained.

DOI: 10.1103/PhysRevC.82.064002 PACS number(s): 11.30.Er, 21.10.Ky, 21.45.Bc, 24.80.+y

I. INTRODUCTION

With the discovery of parity (P) violation, which was suggested by Lee and Yang [1], Landau [2] deduced that charge conjugation and parity (CP) invariance implies that the electric dipole moment (EDM) of particles, for example, the neutron, should be zero. Any CP violation would also imply a corresponding time-reversal (T) invariance violation if the CPT theorem is valid, which is the case for gauge theories. Predating the discovery of parity violation in the weak interaction, Purcell and Ramsey [3] had pointed out that there was no experimental test of parity conservation in the strong interaction. With their student Smith [4], they set limits on the EDM of the neutron of the order of $d_n < 5 \times 10^{-20} e$ cm. The standard model of fundamental interactions predicts values for EDMs (due to second-order W boson exchange) that are significantly smaller than contemporary experiments can detect, of the order of $10^{-31} e$ cm. Therefore, an unambiguous observation of a nonzero EDM at current capabilities would imply a yet-to-be-discovered source of CP violation [5,6]. The new physics could arise in the strong interaction sector (e.g., the θ term) or in the weak interaction sector [e.g., supersymmetric models or left-right (boson mass) symmetry breaking]. Current limits on the nucleon EDM are of the order of $10^{-26} e$ cm. Even if one were to establish a nonzero neutron and proton EDM, those two results would at best determine the isoscalar and isotensor components but would not isolate any isovector component. Thus, one would need a third measurement, such as the deuteron EDM, to fully elucidate the isospin nature of the EDM operator. Both PT-violating and P-conserving, T-violating potentials may give rise to an EDM [5], but one-pion exchange contributes only to the former. We concentrate here upon the effects due to PT invariance violation in the nuclear potential.

The deuteron is attractive as the focus of an EDM investigation, both theoretically and experimentally, because a method has been proposed to directly measure the EDM of charged ions in a storage ring [7–10]. A permanent EDM can arise because a PT-violating interaction can induce a small P-state admixture in the deuteron wave function, one which produces a nonvanishing matrix element of the charge dipole operator $\tau_-^z e\vec{r}$. Although this two-body EDM contribution must be disentangled from the one-body contributions of the neutron and proton, the neutron and proton EDMs tend to cancel in the case of the isospin zero ^{2}H. (If the nucleon EDM were a pure isoscalar as is the case in the θ model, then this cancellation would be exact.) Therefore, the PT-violating nucleon-nucleon (NN) interaction can contribute significantly to the deuteron EDM. Because the deuteron is reasonably understood and has been accurately modeled, reliable calculations are possible. Our purpose is to address the sensitivity of the deuteron EDM to the nuclear physics in the modeling of the nucleon-nucleon interaction. Beyond understanding the model dependence of the ^{2}H EDM, our goal is to determine an appropriate model approximation with which one might reliably calculate the nuclear physics contribution to the ^{3}He and ^{3}H EDMs. Therefore, we examine the uncertainties in the deuteron EDM calculation arising from the short-range repulsion in the ground-state wave function, the dependence on the size of the deuteron D state, and the properties of the $^3P_1$ continuum in intermediate states.

For the purpose of completeness and to place our work in context, we note that Avishai [11] first estimated the two-body deuteron EDM [see Eq. (2)] $d_D^{(2)}$ using a separable potential model due to Mongan [12]. He reported a value of $-0.91\ Ae$ fm when he utilized the physical pion mass for the

*Iraj.Afnan@Flinders.edu.au
†bfgibson@lanl.gov

exchanged meson. [Note: To exclude the PT-violating and strong coupling constants in the one-pion-exchange nucleon-nucleon interaction for the quoted values of the EDM, we have introduced $A = \bar{g}^{(1)}_{\pi \mathrm{NN}} g_{\pi \mathrm{NN}}/(16\pi)$.] However, there is an ambiguity in Avishai's results, in that he states his final result in terms of $A/2$. Because the particular separable potentials used by Avishai were not specified, we were unable to fully confirm his reported numbers. Khriplovich and Korkin [13] later estimated $d_D^{(2)}$ using a zero-range approximation in the chiral limit ($m_\pi \to 0$) and obtained a value of $-0.92\ Ae$ fm. This result does not depend upon the $^3P_1$ interaction and should therefore be directly comparable to our plane-wave result. Finally, using the Argonne and Nijmegen contemporary realistic potential models Av_{18}, Reid93, and Nijm II [14], Liu and Timmermans [15] obtained for the polarization component of the two-body contribution to the deuteron EDM $d_D^{(2)}$ values of $-0.72\ Ae$ fm, $-0.73\ Ae$ fm, and $-0.74\ Ae$ fm, respectively. These relatively model-independent results suggest that pion exchange is indeed the essential aspect of the model. The differing degree of softness of the three potentials at intermediate range correlates with the values for $d_D^{(2)}$, with the Nijm II potential being the softest and producing the largest EDM. The important conclusion for our purpose is that all three models yield essentially the same result; within the range of uncertainty defined by the three models utilized, the value of the polarization component of $d_D^{(2)}$ can be said to be $\approx -0.73 \pm .01\ Ae$ fm. Moreover, Liu and Timmermans estimated that the meson exchange current contribution was substantially smaller, calculated to be less than 5% of the potential model contribution. In any case, our goal is to determine an appropriately simple model with which one can calculate reliably the ^{2}H, ^{3}He, and ^{3}H EDMs, so that our numerical comparisons will be made with the $-0.73 \pm .01\ Ae$ fm value.

II. NUCLEON CONTRIBUTIONS

The total one-body contribution $d_D^{(1)}$ to the deuteron EDM due to the neutron and proton is the sum of the individual nucleon EDMs:

$$d_D^{(1)} = d_n + d_p, \tag{1}$$

whereas the total deuteron EDM is the sum of this one-body contribution and the two-body contribution $d_D^{(2)}$,

$$d_D = d_D^{(1)} + d_D^{(2)} = (d_n + d_p) + d_D^{(2)}. \tag{2}$$

As has been noted, the neutron and proton EDMs can arise from a variety of sources. Because we have nothing new to add to prior analyses of the nucleon EDM, we adopt the approach advanced by Liu and Timmermans [15]:

$$d_D^{(1)} \simeq 0.22 \times 10^{-2} \bar{G}_\pi^{(1)} + O\big(\bar{G}_\pi^{(0,2)}, \bar{G}_{\rho,\omega,\eta}\big), \tag{3}$$

which is expressed in terms of $\bar{G}_X^{(i)}$, the product of the strong coupling constant $g_{X\mathrm{NN}}$ and the associated PT-violating meson-nucleon coupling constant $\bar{g}_X^{(i)}$. (For example, $\bar{G}_\pi^{(1)} = \bar{g}^{(1)}_{\pi \mathrm{NN}} g_{\pi \mathrm{NN}}$.) As noted in Ref. [15], the contributions from the neutron and proton EDMs have a sizable theoretical uncertainty, but the significant cancellation between d_n and d_p is clear. For the two-body contribution to $d_D^{(2)}$, the mean value obtained by Liu and Timmermans can be expressed as

$$d_D^{(2)} = 1.45 \times 10^{-2} \bar{G}_\pi^{(1)}; \tag{4}$$

this corresponds to the EDM value of $-0.73\ Ae$ fm. Hence, for the deuteron there can be little doubt that the nuclear physics contribution to $d_D^{(2)}$ dominates. Even an uncertainty of 50% in $d_D^{(1)}$ contributes only in a minor way. It is the nuclear model aspects of the $d_D^{(2)}$-dominant term in the ^{2}H EDM that we investigate in detail.

III. TWO-BODY CONTRIBUTIONS

The interaction Hamiltonian for the ground state of the system consists of two components: (i) The strong interaction component v based on nucleon-nucleon potentials with parameters adjusted to fit the experimental phase shifts, and (ii) the PT-violating component V, which we parametrize in terms of one-pion exchange with one strong interaction vertex $g_{\pi \mathrm{NN}}$ and a PT-violating vertex $\bar{g}^{(1)}_{\pi \mathrm{NN}}$. As a result, our Hamiltonian takes the form

$$H = H^S + H^{\mathrm{PT}} \quad \text{where} \quad H^S = H_0 + v \quad \text{and} \quad H^{\mathrm{PT}} = V. \tag{5}$$

Because H^{PT} will mix different parity states (i.e., for the deuteron we get coupling between the $^3S_1$–$^3D_1$ large component and the $^3P_1$ small component), we can write the Schrödinger equation for the Hamiltonian in Eq. (5),

$$H|\Psi\rangle = E|\Psi\rangle, \tag{6}$$

as a set of coupled equations of the form

$$(E - H_0)|\Psi_L\rangle = v|\Psi_L\rangle + V|\Psi_S\rangle \tag{7}$$

$$(E - H_0)|\Psi_S\rangle = v|\Psi_S\rangle + V|\Psi_L\rangle, \tag{8}$$

where the total wave function is the sum of the large and small components: $|\Psi\rangle = |\Psi_L\rangle + |\Psi_S\rangle$.

Because $V \ll v$, we have that $V|\Psi_S\rangle \ll v|\Psi_L\rangle$, and we can, to a good approximation, write Eq. (7) as

$$(E - H_0)|\Psi_L\rangle = v|\Psi_L\rangle, \tag{9}$$

which is the Scrödinger equation for the ground state of the system in the absence of the PT-violating interaction. On the other hand, the small component of the wave function $|\Psi_S\rangle$ is given by the solution of Eq. (8) in terms of the amplitude $t(E)$ for the strong potential v as

$$|\Psi_S\rangle = G(E)V|\Psi_L\rangle \quad \text{with} \quad G(E) = G_0(E) + G_0(E)t(E)G_0(E), \tag{10}$$

where $G_0(E) = (E - H_0)^{-1}$ is the free Green's function and $t(E)$ is the amplitude in the partial wave of the small component of the wave function, for example, for the deuteron, $t(E)$ is the amplitude in the $^3P_1$ partial wave at the ground-state energy.

Because the dipole operator

$$O_d = \frac{e}{2} \sum_i \vec{r}_i\ \tau_z(i) \tag{11}$$

is odd under parity, we can write the two-body deuteron EDM ($d_D^{(2)}$) in terms of the total ground-state wave function $|\Psi\rangle = |\Psi_L\rangle + |\Psi_S\rangle$ as

$$d_D^{(2)} = \langle\Psi|O_d|\Psi\rangle = \langle\Psi_L|O_d|\Psi_S\rangle + \langle\Psi_S|O_d|\Psi_L\rangle, \quad (12)$$

where the matrix element of the dipole operator between the small and large component of the wave function can be written in terms of the charge e and the constant A as

$$\begin{aligned}\langle\Psi_L|O_d|\Psi_S\rangle &= \langle\Psi_L|O_d G_0(E)V|\Psi_L\rangle \\ &\quad + \langle\Psi_L|O_d G_0(E)t(E)G_0(E)V|\Psi_L\rangle \quad (13)\\ &\equiv \frac{e}{2}[d_{\rm PW} + d_{\rm MS}]A \quad \text{with} \quad A \equiv \frac{\bar{g}^{(1)}_{\pi{\rm NN}} g_{\pi{\rm NN}}}{16\pi}. \quad (14)\end{aligned}$$

In Eq. (13), the first term on the right-hand side (rhs) involves a complete set of intermediate plane-wave states and is, up to a constant, the plane-wave contribution $d_{\rm PW}$. The second term on the rhs of Eq. (13) involves multiple scattering via the amplitude $t(E)$ and is the multiple-scattering contribution $d_{\rm MS}$. One should note that $E < 0$ is the ground-state energy, and as a result we need the amplitude $t(E)$ at an unphysical point corresponding to the ^{2}H bound-state energy.

IV. NUMERICAL RESULTS

The primary motivations for the present investigation are (i) to determine the sensitivity of $d_D^{(2)}$ to properties of the deuteron (e.g., the D-state probability and the short-range behavior of the deuteron wave function), (ii) to determine the relative importance of $d_{\rm PW}$ and $d_{\rm MS}$—this will suggest the significance of multiple-scattering terms as one proceeds to heavier nuclei, and (iii) to determine the role of the $^3P_1$ interaction in determining the magnitude of $d_{\rm MS}$ and therefore the appropriateness of the $d_{\rm PW}$ approximation in heavier nuclei. Before we proceed to illustrate the sensitivity of the deuteron EDM to nuclear structure effects due to the nuclear interaction, we should detail our choice of nucleon-nucleon interactions and their fit to those aspects of the two-body data relevant to the determination of the EDM.

A. Two-body potentials

The input two-body interactions consists of (i) the PT-violating one-pion-exchange potential, (ii) the deuteron wave function in the absence of the PT-violating interaction, and (iii) the $^3P_1$ interaction that couples to the deuteron $^3S_1$–$^3D_1$ potential as a result of the introduction of the PT-violating potential. The choice of these interactions is motivated by the questions raised regarding the sensitivity of the EDM to nuclear structure effects and the hope of extending the analysis to ^{3}H and ^{3}He using the $d_{\rm PW}$ approximation.

For the PT-violating interaction, we have chosen the standard isovector one-pion exchange given by [16]

$$V = -A[(\vec{\sigma}^{(-)}\cdot\hat{r})\tau_z^{(+)} + (\vec{\sigma}^{(+)}\cdot\tau_z^{(-)})]f(r), \quad (15)$$

where the radial dependence is given by

$$f(r) = -\frac{1}{m_\pi}\frac{d}{dr}\left(\frac{e^{-m_\pi r}}{r}\right), \quad (16)$$

with m_π being the pion mass. Here we have combined the strength of the strong and PT-violating vertices in the constant A given in Eq. (14). This allows us to express the numerical value of the EDM in terms of Ae with e being the charge on the proton. Finally, the spin and isospin operators in Eq. (15) are given by $\vec{\sigma}^{(\pm)} = (\vec{\sigma}^{(1)} \pm \vec{\sigma}^{(2)})$ and $\tau_z^{(\pm)} = (\tau_z^{(1)} \pm \tau_z^{(2)})$.

The strong $^3S_1$–$^3D_1$ interaction basically defines the deuteron wave function. Here we resort to a separable representation of the interaction to simplify the computation when we proceed to the EDM for the three-nucleon system. As a result, the partial-wave expansion of the strong interaction in momentum space is written as

$$\langle\vec{k}|v|\vec{k}'\rangle = \sum_{Sjtm}\sum_{\ell\ell'}\left\langle\hat{k}|\mathcal{Y}^t_{(\ell S)jm}\right\rangle v^{Sjt}_{\ell\ell'}(k,k')\left\langle\mathcal{Y}^t_{(\ell' S)jm}|\hat{k}'\right\rangle, \quad (17)$$

with $|\mathcal{Y}^t_{(\ell S)jm}\rangle$ eigenstates of the orbital angular momentum ℓ, spin S, total angular momentum j, and isospin t. The separability of the potential is defined by the requirement that

$$v^\alpha_{\ell\ell'}(k,k') = g^\alpha_\ell(k)\,\lambda^\alpha_{\ell\ell'}\,g^\alpha_{\ell'}(k'), \quad (18)$$

where $\alpha = (Sjt)$. Here we examine the role of the D-state probability and short-range nature of the nucleon-nucleon interaction. For that we consider two classes of interactions: (i) The first is the Yamaguchi and Yamaguchi (YY) [17] separable potential with 4% and 7% D-state probability. Each has a different D-state probability and no short-range repulsion. (ii) The second is the unitary pole approximation (UPA) [18,19] to the original Reid soft-core potential (Reid68) [20] and the Nijmegen modified Reid potential (Reid93) [14]. The UPA potential by definition generates the same deuteron wave function as the original potential [19] that provided the optimum fit to the available data at the time the potentials were constructed and includes short-range repulsion. In addition, the models have different D-state probabilities for the deuteron.

For the Yamaguchi and Yamaguchi potentials [17], the form factor $g^\alpha_\ell(k)$ is given by

$$g_\ell(k) = \frac{k^\ell}{\left(k^2+\beta_\ell^2\right)^{(\ell+2)/2}}, \quad (19)$$

where the parameters β_ℓ and $\lambda_{\ell\ell'}$ are detailed in Table I. Also included in this table are the binding energy ϵ_D and the quadrupole moment Q_D for these two potentials.

In constructing the UPA to the Reid68 [20] and Reid93 potentials [14], we have used the method of moments [19] to solve the Schrödinger equation for the deuteron wave function

TABLE I. Parameters for the Yamaguchi-Yamaguchi potentials [17] with 4% and 7% D-state probability for the deuteron. Also included are the binding energy and quadrupole moments.

D state	β_0	β_2	λ_{00}	λ_{02}	λ_{22}	ϵ_D (MeV)	Q_D
4%	1.3134	1.5283	−0.6419	1.0849	−1.8320	2.2234	0.2821
7%	1.2410	1.9480	−0.3776	1.6975	−7.6301	2.2265	0.2826

TABLE II. The strength $\lambda_{\ell\ell'}$ for the UPA approximation to the Reid68 [20] and Reid93 [14] potentials.

Potential	λ_{00}	λ_{02}	λ_{22}
Reid68	$-5.289\,672\,5 \times 10^{-2}$	$-2.438\,578\,6$	$1.185\,092\,6$
Reid93	$-4.770\,478\,9 \times 10^{-1}$	$-1.811\,176\,4$	$2.582\,546\,7 \times 10^{-1}$

in coordinate space using the original potentials. This was achieved by taking the form factors such that the resultant deuteron wave functions for the Reid68 and Reid93 potentials are linear combinations of the Yamaguchi-Yamaguchi-type wave functions with different range parameters β_i and therefore are of the form

$$g_\ell(k) = \sum_{i=1}^{12} \frac{c_\ell^i\, k^\ell}{\left(k^2 + \beta_i^2\right)^{(\ell+2)/2}}. \tag{20}$$

The strengths of the UPA potential ($\lambda_{\ell\ell'}$), adjusted to reproduce the matrix elements of the original Reid68 and Reid93 potentials, are given in Table II, while the parameters of the UPA form factors β_i and c_ℓ^i for $\ell = 0$ and 2 are given in Table III. Here, we have chosen the range parameters β_i to be multiples of the pion mass with the hope of reproducing some of the analytic structure of the one pion tail in the original Reid potentials.

To establish the quality of the UPA deuteron wave function generated using the method of moments, we present in Table IV the deuteron properties for the original potential and the UPA for both Reid68 and Reid93 potentials. Also included are the effective range parameters to illustrate the domain of agreement in the scattering amplitude between the original and the UPA potential. It is clear from these results that the method of moments gives a very good representation of the original deuteron wave function and can reproduce the effective range parameters.

Finally, to examine the importance of multiple scattering in determining the deuteron EDM, we need to introduce a $^3P_1$ interaction to calculate $d_{\rm MS}$. Here we need to know the importance of the fit to the data and the role of the off-shell amplitude in determining the magnitude of $d_{\rm MS}$. To simplify the evaluation of $d_{\rm MS}$, we have chosen to use separable potentials with different form factors. The Mongan [12] potentials used by Avishai [11] come with different form factors and therefore different off-shell properties. They are either rank 1 or rank 2 to optimize the fit to the data; that is, the potentials are of the form

TABLE IV. Comparison of the deuteron properties for the original potential and the UPA potential for both Reid68 and Reid93 potentials. Tabulated are the binding energy ϵ_D, the asymptotic S-wave normalization A_S, the ratio η of the asymptotic D wave to S wave, the quadrupole moment Q_D, and the D-state probability P_D. Also included are the scattering length a_t and effective range r_t.

	Reid68		Reid93	
	UPA	Original	UPA	Original
ϵ_D	2.2246	2.2246	2.2246	2.2246
A_S	0.87893	0.87758	0.8863	0.8853
$\eta = A_D/A_S$	0.026556	0.026223	0.02565	0.0251
Q_D	0.2800	0.27964	0.2709	0.2703
P_D	6.4691	6.4696	5.699	5.699
a_t	5.408	5.390	5.445	5.422
r_t	1.752	1.720	1.799	1.755

$$v_{^3P_1}(k,k') = \sum_{i=1}^{n} g_i(k)\lambda_i g_i(k'), \tag{21}$$

where $n = 1$ for rank 1 potentials and $n = 2$ for rank 2 potentials. For the form factors $g_i(k)$, we use the four different forms chosen by Mongan (see Table V). Considering the fact that Mongan adjusted the parameters of his potentials to fit the Livermore data of the 1960s, we first need to compare the phase shifts predicted by the Mongan potentials and those that we constructed to fit the latest Nijmegen [21] neutron-proton (np) data. In Fig. 1, we compare the $^3P_1$ phase shifts for rank 1 and rank 2 case I form factors for Mongan's potentials with those refitted to the Nijmegen data. Also included are the Nijmegen [21] np phase shifts. It is clear from the the results

TABLE III. The form factor parameters of the UPA approximation to the Reid68 [20] and Reid93 [14] potentials.

i	β_i (fm^{-1})	Reid68		Reid93	
		c_0^i	c_2^i	c_0^i	c_2^i
1	0.7	$7.211\,864\,19 \times 10^{-3}$	$-2.244\,570\,73 \times 10^{-3}$	$6.306\,467\,24 \times 10^{-3}$	$-3.088\,931\,40 \times 10^{-3}$
2	1.4	$1.788\,266\,42 \times 10^{-1}$	$-3.310\,630\,31 \times 10^{-1}$	$2.128\,465\,33 \times 10^{-1}$	$-3.015\,648\,84 \times 10^{-1}$
3	2.1	$1.312\,606\,92$	$-1.047\,452\,93$	$6.054\,506\,38$	$-1.781\,855\,16$
4	2.8	$2.134\,304\,24$	$-1.436\,280\,43$	$-2.577\,778\,24 \times 10^{1}$	$7.870\,427\,55 \times 10^{-1}$
5	4.2	$1.465\,788\,61 \times 10^{2}$	$-1.956\,952\,56 \times 10^{1}$	$3.200\,797\,33 \times 10^{2}$	$-2.534\,838\,26 \times 10^{1}$
6	5.6	$-8.103\,877\,28 \times 10^{2}$	$3.127\,821\,73$	$-1.491\,743\,73 \times 10^{3}$	$4.673\,872\,61 \times 10^{1}$
7	7.0	$1.129\,345\,49 \times 10^{3}$	$1.511\,269\,63 \times 10^{2}$	$2.327\,460\,50 \times 10^{3}$	$3.379\,085\,96 \times 10^{1}$
8	9.8	$-5.877\,797\,28 \times 10^{2}$	$-4.267\,019\,86 \times 10^{2}$	$-2.574\,026\,58 \times 10^{3}$	$-2.103\,535\,62 \times 10^{2}$
9	12.6	$-2.276\,385\,08 \times 10^{2}$	$5.923\,980\,37 \times 10^{2}$	$2.532\,234\,23 \times 10^{3}$	$3.414\,120\,20 \times 10^{2}$
10	15.4	$5.337\,848\,64 \times 10^{2}$	$-3.735\,331\,99 \times 10^{2}$	$-1.312\,465\,53 \times 10^{3}$	$-2.421\,261\,56 \times 10^{2}$
11	21.0	$-2.537\,461\,05 \times 10^{2}$	$9.684\,007\,08 \times 10^{1}$	$2.663\,299\,30 \times 10^{2}$	$7.606\,099\,41 \times 10^{1}$
12	26.6	$6.638\,700\,56 \times 10^{1}$	$-2.095\,137\,06 \times 10^{1}$	$-4.841\,064\,37 \times 10^{1}$	$-1.899\,791\,13 \times 10^{1}$

TABLE V. The parameters of the new rank 1 and rank 2 potentials with the different Mongan form factors. The parameters are adjusted by minimizing the χ^2 defined in Eq. (22), taking the experimental phases from the latest Nijmegen [21] *np* phase-shift analysis. The form factor for case III is written in terms of $Q_1(\xi)$, the Legendre function of the second kind.

Potential	Form factor $g_i(k)$	Rank	β_1	λ_1	β_2	λ_2	χ^2
Case I	$k/(k^2+\beta_i^2)$	1	1.725	0.95			0.62
		2	0.90	0.059	3.58	−2.0	0.02
Case II	$k/(k^2+\beta_i^2)^{3/2}$	1	2.38	9.35			0.81
Case III	$\left[\frac{1}{k^2\pi}Q_1\left(1+\frac{\beta_i^2}{2k^2}\right)\right]^{1/2}$	1	1.68	60.0			0.19
		2	1.20	120.0	4.4	−2.3	0.12
Case IV	$k/(k^2+\beta_i^2)^2$	1	2.715	147.0			0.78

in Fig. 1 that the original Mongan potentials give a poor fit to the current data, while the new fits reproduce the data to a much better degree. Since the $^3P_1$ amplitude required for the determination of $d_{\rm MS}$ is evaluated at the deuteron binding energy (i.e., *below* the elastic threshold), it is essential that we fit well the low-energy phase shifts. Because these are small, we have chosen the criteria for a good fit χ^2 defined as

$$\chi^2 = \sum_{i=1}^{n} \frac{\left|\delta_i^{\rm th} - \delta_i^{\rm exp}\right|^2}{\left|\delta_i^{\rm exp}\right|^2}, \tag{22}$$

where $n = 11$ is the number of data points below 300 MeV. In Table V, we present new fits to the Nijmegen *np* data for the different form factors used by Mongan.[1] Included are rank 1 and rank 2 potentials and the χ^2 for each potential. It is clear from the χ^2 that the rank 2 potentials give a better fit. This is especially true for the case I form factor. In the following discussion of the deuteron EDM, we consider these different $^3P_1$ potentials to establish the importance of fitting the data and the role of the off-shell behavior of the amplitude.

B. The deuteron EDM

We now turn to the study of the sensitivity of the deuteron EDM to the nuclear structure effects as defined by the strong nucleon-nucleon interactions detailed previously. We first consider the sensitivity of the two-body deuteron EDM $d_D^{(2)}$ to the D-state probability (P_D). In Table VI, we summarize the contributions to the deuteron EDM for the four different deuteron wave functions being considered. For the $^3P_1$ interaction, we use a rank 2 Mongan case I potential (fitted to the latest Nijmegen phase shifts [21]). Also included are the results of Khriplovich and Korkin [13]. We observe that in the plane-wave approximation ($d_{\rm PW}$) there is little variation with P_D, and the short-range repulsion incorporated in the two Reid potential wave functions provides no more than a 10% reduction in $d_{\rm PW}$. Moreover, the results are effectively consistent with the zero-range (chiral limit) approximation of Khriplovich and Korkin. In particular, the plane-wave results for the two YY models suggest that the dependence upon the deuteron D-state probability is such that an S-state deuteron result would approach that of Ref. [13]. In contrast, the multiple-scattering contribution ($d_{\rm MS}$), which is of the opposite sign of the plane-wave term, varies considerably depending upon the short-range character of the deuteron wave function. In particular, the two Reid potentials with different P_D values yield quite similar values of $d_{\rm MS}$, but these are only half those generated by the YY potentials. The difference between the YY and Reid potential models can be understood in light of our knowledge that there is no explicit short-range repulsion in the YY potentials. We return to this difference when we address the role of the off-shell behavior of the $^3P_1$ amplitude in determining the magnitude of the multiple-scattering contribution $d_{\rm MS}$. From these results, we may conclude that the strong repulsion at short distance in realistic nucleon-nucleon potentials reduces the effects of multiple scattering in the matrix element to such an extent that the multiple-scattering contribution $d_{\rm MS}$ is only

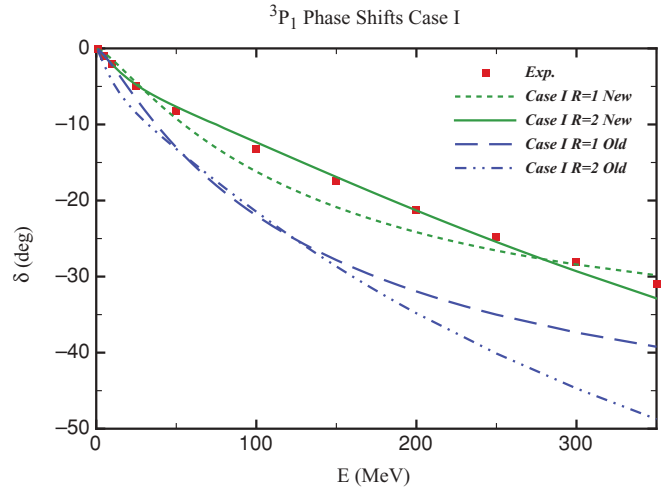

FIG. 1. (Color online) Comparison of the $^3P_1$ phase shifts for the Mongan potentials (old) with case I form factor and rank 1 ($R = 1$) and rank 2 ($R = 2$) with the new fit (new) and the experimental (Exp.) Nijmegen [21] *np* data.

[1]The case III form factor was motivated by the observation that the on-shell Born amplitude for a rank 1 separable potential is identical to the on-shell Born amplitude resulting from meson exchange potential with a meson mass β_1.

TABLE VI. The variation of the two-body EDM with D-state probability of the deuteron. For the $^3P_1$ interaction. we use the new fit case I rank 2 potential. Also included are the results of Khriplovich and Korkin [13].

$^3S_1$–$^3D_1$	P_d	$d_{\rm PW}(A\ e\ {\rm fm})$	$d_{\rm MS}(A\ e\ {\rm fm})$	$d_D^{(2)}(A\ e\ {\rm fm})$
YY 4%	4%	−1.035	0.411 5	−0.623 4
Reid93	5.7%	−0.971 5	0.200 9	−0.770 6
Reid68	6.5%	−0.962 0	0.171 8	−0.790 2
YY 7%	7%	−1.083	0.427 1	−0.656 4
Khriplovich *et al.*		−0.92		

about 20% of the plane-wave contribution $d_{\rm PW}$. Furthermore, as noted previously, the final results are not particularly sensitive to P_D.

To establish the importance of the multiple-scattering contribution ($d_{\rm MS}$) to the total two-body deuteron EDM, we turn to the dependence of $d_D^{(2)}$ on the choice of the $^3P_1$ interaction. First we need to examine the sensitivity of the multiple-scattering contribution to the $^3P_1$ phase shifts. This can be achieved by comparing the results for the EDM using the old Mongan fit to the 1960s Livermore phase-shift analysis and the new fit with the same separable potential form factors to the latest Nijmegen [21] np data. We have in Table VII the EDM results for the rank 1 separable potentials with case I and III form factors. For the deuteron wave function, we have used either the UPA to the Reid68 or the YY 4% potentials. It is clear from these results that the multiple-scattering contribution ($d_{\rm MS}$) is reduced as a result of the fit to the more recent phase-shift analysis (compare rows 4 and 5 or rows 6 and 7 in Table VII). This reduction in $d_{\rm MS}$ is consistent with the observation that the new $^3P_1$ potentials provide less repulsion (i.e., smaller phase shifts; see Fig. 1) and, therefore, substantially smaller multiple-scattering contributions than the old fits due to Mongan. This observation is encouraging for extending the analysis based on $d_{\rm PW}$ to the three-nucleon EDM, as the new np data suggest a reduced contribution from the multiple-scattering term.

We now return to the role of the short-range repulsion in the deuteron wave function on the magnitude of the multiple-scattering term $d_{\rm MS}$ as illustrated in Table VI. In comparing the results for the Reid68 and 4% YY deuterons (columns 3 and 5 in Table VII) for the case I and case III $^3P_1$ potentials, we find that the multiple-scattering term is suppressed for both $^3P_1$ potentials. This suggests that the effect tabulated in Table VI might be valid in general, which implies that the inclusion of multiple scattering will require a more realistic treatment of the deuteron wave function than is the case for the zero-range approximation employed by Khriplovich and Korkin [13]. In fact, for some combination of deuteron wave function and $^3P_1$ interaction (4% YY and case III old), the multiple-scattering contribution ($d_{\rm MS}$) is about the same size as the plane-wave approximation ($d_{\rm PW}$) and as a result the deuteron EDM $d_D^{(2)}$ is suppressed by an order of magnitude compared to the combination Reid68 and case I new.

TABLE VII. Variation in the deuteron EDM with changes in the np phase shifts for two rank 1 separable potentials having different form factors as defined by Mongan [12]. Here "new" refers to the fit to the latest Nijmegen [21] np phase shifts while "old" refers to the original Mongan fit.

$^3S_1$–$^3D_1$		Reid68 $d_{\rm PW} = -0.96$		YY 4% $d_{\rm PW} = -1.04$	
Case	χ^2	$d_{\rm MS}$	$d_D^{(2)}$	$d_{\rm MS}$	$d_D^{(2)}$
I (new)	0.62	0.21	−0.75	0.57	−0.47
I (old)	1.90	0.31	−0.66	0.78	−0.26
III (new)	0.19	0.25	−0.71	0.77	−0.27
III (old)	6.67	0.42	−0.54	1.16	0.12

We now turn to the role of the off-shell behavior of the $^3P_1$ amplitude in the deuteron EDM. Here again we make use of the different separable potentials with the different form factors used by Mongan after readjusting the parameters of the potential to fit the latest Nijmegen [21] np phase shifts. The parameters of these new potentials are given in Table V. In Table VIII, we report the multiple-scattering contribution $d_{\rm MS}$ and the two-body EDM $d_D^{(2)}$ for these separable potentials. In each case, we have made use of either the Reid93 or 4% YY deuteron wave functions in the calculations. Here we observe that for the Reid93 deuteron there is a smaller variation in $d_D^{(2)}$ than is the case for the 4% YY deuteron. This is due to the fact that the multiple-scattering contributions, $d_{\rm MS}$, for the 4% YY deuteron have a substantially larger variation for the different fits to the np data. This is consistent with the results in Table VII and is due to the absence of short-range repulsion in the YY potentials. Here we can raise a number of questions regarding the role of the $^3P_1$ amplitude in determining the magnitude of the multiple-scattering contribution $d_{\rm MS}$. These are as follows:

- Why is $d_{\rm MS}$ almost a factor of two smaller for the Reid93 potential when compared to that for the 4% YY potential?
- Why, for the Reid93 deuteron, is $d_{\rm MS}$ about the same for all form factors with the possible exception of case III, which gives the largest contribution?
- Why is it that for the 4% YY deuteron $d_{\rm MS}$ has a much larger variation than is the case for Reid93?

To address these questions and to try to correlate the results in Table VIII with the off-shell behavior of the $^3P_1$ amplitude, we need to examine the analytic continuation of the P-wave-scattering wave function to the deuteron pole. This is defined in momentum space in terms of the half off-shell t matrix as

$$\begin{aligned}\psi_\alpha(k) &= G_0(-\epsilon_D, k)\, t_\alpha(k, i\kappa; -\epsilon_D) \\ &= G_0(-\epsilon_D, k)\, \mathbf{g}_\alpha(k)\boldsymbol{\tau}_\alpha(-\epsilon_D)\mathbf{g}_\alpha^\dagger(i\kappa) \\ &\equiv \Psi_\alpha(k)\boldsymbol{\tau}_\alpha(-\epsilon_D)\mathbf{g}_\alpha^\dagger(i\kappa), \end{aligned} \tag{23}$$

where α labels the $^3P_1$ channel, $\epsilon_D = \frac{\kappa^2}{2\mu}$ is the binding energy of the deuteron, and μ is the np reduced mass. Here, the free Green's function at the deuteron energy is given by $G_0(-\epsilon_D, k) = -(2\mu)(\kappa^2 + k^2)^{-1}$, while the amplitude $t_\alpha(k, i\kappa; -\epsilon_D)$ is the half off-shell $^3P_1$ t matrix evaluated at the deuteron pole. In the second line of Eq. (23), we have

TABLE VIII. The dependence of $d_{\rm MS}$ on the $^3P_1$ separable potential form factor as defined by Mongan [12] and that are fit to the latest np phase shifts. The Reid93 or the 4% YY deuteron wave function is used in all cases as indicated.

Case	Rank	χ^2	Reid93 $d_{\rm PW} = -0.9715$		YY 4% $d_{\rm PW} = -1.035$	
			$d_{\rm MS}(A\ e\ {\rm fm})$	$d_D^{(2)}(A\ e\ {\rm fm})$	$d_{\rm MS}(A\ e\ {\rm fm})$	$d_D^{(2)}(A\ e\ {\rm fm})$
I	1	0.62	0.258 3	−0.713 2	0.566 5	−0.468 4
I	2	0.02	0.200 9	−0.770 6	0.411 5	−0.623 4
II	1	0.81	0.222 9	−0.748 6	0.380 7	−0.654 2
III	1	0.19	0.307 5	−0.664 0	0.765 4	−0.269 6
III	2	0.12	0.380 5	−0.591 0	1.108	0.073 4
IV	1	0.78	0.215 3	−0.756 2	0.327 7	−0.707 2

written the off-shell t matrix in its separable form with

$$\boldsymbol{\tau}_\alpha(-\epsilon_D) = \left[\boldsymbol{\lambda}_\alpha + 2\mu \int_0^\infty dk k^2 \, \frac{\mathbf{g}_\alpha^\dagger(k)\mathbf{g}_\alpha(k)}{\kappa^2 + k^2}\right]^{-1}. \quad (24)$$

For rank 1 potentials, $\boldsymbol{\tau}_\alpha(-\epsilon_D)$ is positive definite since the potential is repulsive (i.e., $\lambda_\alpha > 0$). As a result, the scattering wave function can be written as

$$\psi_\alpha(k) = \chi_\alpha(k)\sqrt{\tau_\alpha(-\epsilon_D)}\, g_\alpha(i\kappa). \quad (25)$$

This definition of the function $\chi_\alpha(k)$ is motivated in the following discussion of the matrix elements of the dipole operator O_d and the PT-violating one-pion-exchange potential V that go into the evaluation of $d_{\rm MS}$.

In Fig. 2, we plot the function $\chi_\alpha(k)$ for all the rank 1 potentials used in Table VIII. A careful inspection of this figure reveals that (i) the scattered function $\chi_\alpha(k)$ for the case III form factor is substantially larger for $k < 1.0$ fm^{-1} than that of the other three form factors, and (ii) for $k > 3$ fm^{-1} the case III scattered function has the longest range followed by case I, case II, and finally case IV. This is clear from the choice of form factors as given in Table V.

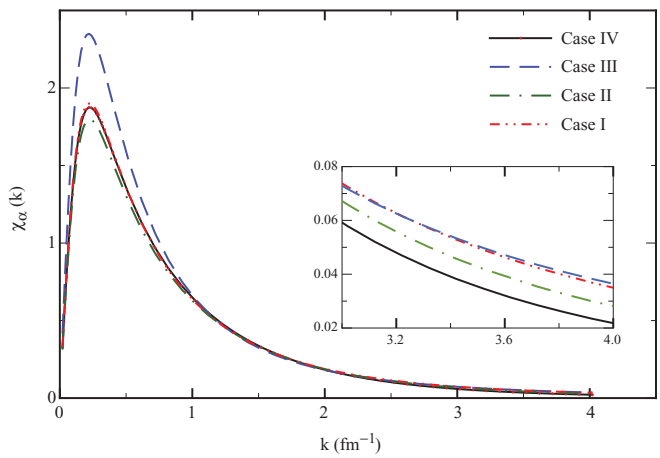

FIG. 2. (Color online) Comparison of the $^3P_1$ scattered function $\chi_\alpha(k)$ defined in Eq. (25) for the rank 1 separable potentials that fit the latest Nijmegen [21] np phase shifts.

To establish how this momentum dependence of the $^3P_1$ scattered function affects the multiple-scattering contribution $d_{\rm MS}$ to the deuteron EDM, we recall from Eq. (14) that $d_{\rm MS}$ can be written as

$$d_{\rm MS} = -2[\mathbf{O}_{sp} + \mathbf{O}_{dp}]\boldsymbol{\tau}(-\epsilon_D)[\mathbf{V}_{ps} + \mathbf{V}_{pd}], \quad (26)$$

where

$$\mathbf{O}_{D\alpha} = \langle\Psi_D|O_d|\Psi_\alpha\rangle \quad \text{and} \quad \mathbf{V}_{\alpha D} = \langle\Psi_\alpha|V|\psi_D\rangle, \quad (27)$$

with $D = {}^3S_1$ or $^3D_1$ and $\alpha = {}^3P_1$. For rank 1 separable potentials, we can absorb a factor of $\sqrt{\tau(-\epsilon_D)}$ into the matrix elements, that is, $\mathcal{O}_{\alpha p} \equiv O_{\alpha\beta}\sqrt{\tau(-\epsilon_D)}$ and $\mathcal{V}_{p\alpha} \equiv \sqrt{\tau(-\epsilon_D)}V_{p\alpha}$, and therefore for rank 1 potentials we have

$$d_{\rm MS} = -2[\mathcal{O}_{sp} + \mathcal{O}_{dp}][\mathcal{V}_{ps} + \mathcal{V}_{pd}]. \quad (28)$$

The values of $\mathcal{O}_{\alpha p}$ and $\mathcal{V}_{p\alpha}$ for the four different form factors and with a deuteron wave function given by either the 4% YY or the Reid93 potentials are presented in Table IX. It is clear from these results that the matrix elements of the dipole operator O_d, which is long range in coordinate space, are to a good approximation independent of the deuteron wave function and to within 20% independent of the $^3P_1$ potential. On the other hand, the matrix elements of the PT-violating one-pion-exchange potential, which probes the short-range behavior of both the $^3P_1$ and the deuteron wave function, are clearly model dependent. In particular, for the Reid93 deuteron

TABLE IX. The matrix elements of the dipole operator O_d and the PT-violating one-pion-exchange potential V for the four different form factors and two different deuteron wave functions.

Deuteron	Case	$\mathcal{O}_{sp}$	$\mathcal{O}_{dp}$	$\mathcal{V}_{ps}$	$\mathcal{V}_{pd}$
4% YY	I	−0.419 7	−0.055 99	0.553 3	0.042 11
	II	−0.403 9	−0.054 22	0.379 4	0.036 18
	III	−0.481 9	−0.063 00	0.657 8	0.044 44
	IV	−0.418 5	−0.056 22	0.312 4	0.032 76
Reid93	I	−0.422 1	−0.060 69	0.216 9	0.090 31
	II	−0.406 8	−0.059 06	0.192 8	0.046 41
	III	−0.485 2	−0.067 12	0.226 9	0.051 54
	IV	−0.422 4	−0.061 05	0.179 3	0.043 38

with short-range repulsion, the variation in $\mathcal{V}_{p\alpha}$ is small with the case III form factor giving the largest contribution and case IV yielding the smallest contribution, followed by cases II and I. This is consistent with the observation made in the Fig. 2 insert regarding the asymptotic behavior of the function $\chi_\alpha(k)$. This is also consistent with the observation in Table VIII for rank 1 potentials. On the other hand, for the 4% YY deuteron, with no short-range repulsion, the matrix elements are almost a factor of two larger with the case III form factor giving the largest contribution and case IV the smallest. From the results in Table IX, we may conclude that it is the matrix element of the PT-violating one-pion-exchange potential that probes the short-range behavior of the $^3P_1$ and deuteron wave functions and, as a result, determines the magnitude of $d_{\rm MS}$. To that extent, it is essential that one generate those two wave functions in a consistent frame work. On the other hand, when the deuteron includes the short-range behavior dictated by modern nucleon-nucleon interactions, the contribution of the multiple-scattering term $d_{\rm MS}$ is suppressed ($\approx$20%) in comparison to the plane-wave contribution $d_{\rm PW}$. This suggests that one may be able to evaluate the EDM for the three-nucleon system in the plane-wave approximation in such a model with an error of the order of 20%.

Finally, the results in Table IX for $\mathcal{O}_{\alpha p}$ and $\mathcal{V}_{p\alpha}$ indicate that the contributions from the D-wave component of the deuteron wave function are an order of magnitude smaller than those of the S-wave component. This may suggest that one could neglect the D-wave component in calculating $d_{\rm MS}$ and a simplification of the calculation of the multiple-scattering term in heavier nuclei. This observation is consistent with the results in Table VI where the multiple-scattering contribution has a variation of about 10% with D-state probability.

V. CONCLUSIONS

From our analysis, we offer the following conclusions: (i) In the absence of multiple scattering ($d_{\rm MS} = 0$), the variation in $d_D^{(2)}$ due to differences in the deuteron wave functions is less than 5%, and the value of $d_{\rm PW}$ is consistent with the zero-range (chiral limit) results of Khriplovich and Korkin [13]. (ii) The contribution from multiple scattering $d_{\rm MS}$ is sensitive to the short-range behavior of the deuteron wave function, and the $d_{\rm MS}$ contribution is about 20% for realistic parametrizations of the deuteron such as those represented by the Reid93 potential model. This suggests that we can extend the analysis to heavier nuclei in the plane-wave approximation with an estimated error of $\approx$20%. (iii) As suggested by Liu and Timmermans, one pion exchange dominates the deuteron EDM calculation. (iv) The contribution from the $^3P_1$ interaction via $d_{\rm MS}$ depends on the phase shifts in this channel as well as the off-shell behavior of the amplitude. (v) A comparison of our Reid93 results with those of Liu and Timmermans [15] indicates that one can use a separable potential approximation in heavier nuclei, for example, ^{3}He and ^{3}H, with minimal loss in accuracy. Moreover, until deuteron EDM experiments attain an uncertainty of less than 10%, simple separable potential model calculations should provide an adequate description.

ACKNOWLEDGMENT

The work of B.F.G. was performed under the auspices of the National Nuclear Security Administration of the US Department of Energy at Los Alamos National Laboratory under Contract No. DE-AC52-06NA25396.

[1] T. D. Lee and C. N. Yang, Phys. Rev. **104**, 254 (1956).
[2] L. Landau, Nucl. Phys. **3**, 127 (1957).
[3] E. M. Purcell and N. F. Ramsey, Phys. Rev. **78**, 807 (1950).
[4] J. H. Smith, E. M. Purcell, and N. F. Ramsey, Phys. Rev. **108**, 120 (1957).
[5] P. Herczeg, *Symmetries and Fundamental Interactions in Nuclei*, edited by W. C. Haxton and E. M. Henley (World Scientific, Singapore, 1995), pp. 89–125.
[6] I. B. Khriplovich and S. K. Lamoreaux, *CP Violation without Strangeness: Electric Dipole Moments of Particles, Atoms, and Molecules* (Springer-Verlag, Berlin, 1997).
[7] I. B. Khriplovich, Phys. Lett. B **444**, 98 (1998).
[8] F. J. M. Farley, K. Jungmann, J. P. Miller, W. M. Morse, Y. F. Orlov, B. L. Roberts, Y. K. Semertzidis, A. Silenko, and E. J. Stephenson, Phys. Rev. Lett. **93**, 052001 (2004).
[9] Y. K. Semertzidis *et al.*, AIP Conf. Proc. **698**, 200 (2004).
[10] Y. F. Orlov, W. M. Morse, and Y. K. Semertzidis, Phys. Rev. Lett. **96**, 214802 (2006).
[11] Y. Avishai, Phys. Rev. D **32**, 314 (1985).
[12] T. R. Mongan, Phys. Rev. **175**, 1260 (1968); **178**, 1597 (1969).
[13] I. B. Khriplovich and R. V. Korkin, Nucl. Phys. A **665**, 365 (2000).
[14] V. G. J. Stoks, R. A. M. Klomp, C. P. F. Terheggen, and J. J. de Swart, Phys. Rev. C **49**, 2950 (1994).
[15] C.-P. Liu and R. G. E. Timmermans, Phys. Rev. C **70**, 055501 (2004).
[16] P. Herczeg, Hyperfine Interact. **75**, 127 (1992).
[17] Y. Yamaguchi and Y. Yamaguchi, Phys. Rev. **95**, 1635 (1954).
[18] I. R. Afnan and J. M. Read, Aust. J. Phys. **26**, 725 (1973).
[19] I. R. Afnan and J. M. Read, Phys. Rev. C **12**, 293 (1975).
[20] R. V. Reid, Ann. Phys. (NY) **50**, 411 (1968).
[21] V. G. J. Stoks, R. A. M. Klomp, M. C. M. Rentmeester, and J. J. de Swart, Phys. Rev. C **48**, 792 (1993).